Journal of
Synchrotron
Radiation

ISSN 0909-0495

Received 17 August 2004
Accepted 8 November 2004

On the imaging of the flux-line lattice of a type-II superconductor by soft X-ray absorption microscopy

M. Fähnle,[a]* J. Albrecht,[a] T. Eimüller,[a] P. Fischer,[b] E. Goering,[a] D. Steiauf[a] and G. Schütz[a]

[a]Max-Planck-Institut für Metallforschung, Heisenbergstrasse 3, 70569 Stuttgart, Germany, and [b]Center for X-ray Optics, E. O. Lawrence Berkeley National Laboratory, MS-400, 1 Cyclotron Road, Berkeley, CA 94720, USA. E-mail: faehnle@mf.mpg.de

A new method is proposed for the imaging of the flux-line lattice of a type-II superconductor by soft X-ray absorption microscopy. It is shown that the method is very demanding but probably realisable in the foreseeable future. The new method has the potential to image in real space static and dynamical properties of the flux-line lattice at arbitrary external fields and with single-flux-line resolution.

Keywords: X-ray absorption microscopy; flux-line lattice.

1. Introduction

When the magnetic field H_{ext} applied to a type-II superconductor exceeds the lower critical field H_{c1}, single flux lines (FL) enter the sample. Close to the centre of the FL there is a magnetic field which decays into the surrounding superconducting matrix with a characteristic length, the penetration depth λ. Furthermore, at the centre the superconducting order parameter ω is zero, and it increases with increasing distance within a range described by the coherence length ξ. With increasing H_{ext} the various FL come more and more close and form a flux-line lattice (FLL), and at the upper critical field H_{c2} bulk-superconductivity breaks down.

Imaging of the FLL has regained great interest after the discovery of high-temperature superconductors which exhibit new vortex phenomena like formation of vortex glasses, melting of the FLL and rapid creep of FLs (Blatter *et al.*, 1994). To investigate these phenomena, static and dynamical imaging of the FLL is very helpful, especially real-space imaging techniques (as contrasted to Bragg scattering techniques in reciprocal space) which allow the observation of the individual FLs. Thereby, the various techniques may be subdivided into two groups (for an excellent review, see Bending, 1999). The representatives of the first group (decoration techniques, electron microscopy, magnetic force microscopy, scanning Hall probe microscopy and magneto-optical imaging) visualize the variation of the magnetic field across the sample due to the FLL. In contrast, scanning tunneling microscopy (STM; de Lozanne, 1999) is sensitive to the spatial variation of ω. For high-temperature superconductors, λ (100–200 nm) is about two orders of magnitude larger than ξ (1–2 nm). Thus the relative variation of the magnetic field originating from the overlap of individual FLs in the FLL is much smaller than that of ω (Brandt, 1997). Therefore, techniques belonging to the first group are confined to a very small field range around H_{c1}, whereas the STM can also be used for higher fields. A disadvantage of the latter technique is that it often struggles with the problem of preparing appropriate surfaces which is manifest in several high-T_c superconductors. For dynamical imaging the magneto-optical technique may be used; however, only at low fields and with limited spatial resolution.

In the present paper we suggest to image the FLL by soft X-ray microscopy, which is sensitive to ω and thus may be used also at higher fields as the STM, with the advantage of less stringent demands for appropriate surfaces. The spatial resolution of the new technique is less than that of STM but high enough to resolve the individual FLs even at higher fields. It also has the potential to image the dynamical properties of the FLL. So far, dynamical imaging has been performed mainly by magneto-optical techniques with their limited spatial resolution. The new method therefore in principle combines the advantages of the STM (high resolution, applicability at high fields) and the magneto-optical methods (dynamical imaging) while avoiding their disadvantages (critical surface preparation and limited spatial resolution, respectively).

2. Basic idea

Irradiating the superconducting solid with X-rays of energy E slightly above the absorption edge $E_F - E_c$ (E_F is the Fermi energy), electrons are excited from core states (with energy E_c) and deposited into unoccupied quasiparticle states of the valence band of the solid. This generates an absorption line with finite linewidth $\delta E = 2\Gamma$. In the normal-conducting FL core of a conventional superconductor the quasiparticle density of states $n^n(E)$ can often be taken as a constant for an energy range comparable with 2Γ. In contrast, the quasiparticle density $n^s(E)$ in the superconducting matrix has a gap of width 2Δ around E_F with a peak or even a singularity at the gap edges (Fig. 1). Furthermore, in the normal-conducting FL core there is a

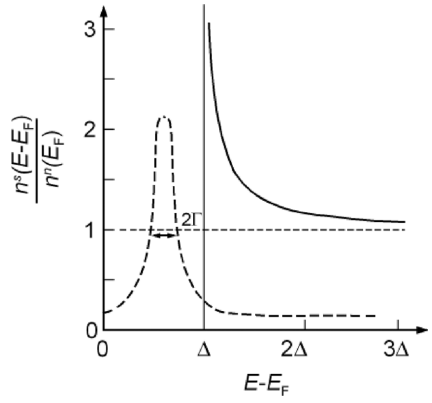

Figure 1
Schematic representation of the quasiparticle density of states for the normal-conducting material (n^n, horizontal broken line) and for the superconducting material (n^s, full line) close to the Fermi energy E_F. The broken curve represents a Lorentzian broadening function.

spin-splitting of $n^n(E)$ induced by the magnetic field in the FL. For materials with large $1/\xi$ the magnetic fields of the individual FLs overlap very strongly for H_{ext} not very close to H_{c1} (see §1), and then $n^s(E)$ is also influenced by the magnetic field. For simplicity, we first neglect the spin splitting and we assume that Γ is much smaller than Δ. When we then irradiate the material with an energy in the range $E_F - E_c < E < E_F - E_c + \Delta$, we can excite only the electrons in the normal-conducting FL core because in the superconducting matrix there are no available quasiparticle states in that energy range (Fig. 1). The resulting absorption contrast between the FL cores and the superconducting matrix could be used to image the FLL. When irradiating with an energy slightly larger than $E_F - E_c + \Delta$, the absorption in the superconducting matrix could be larger than that in the FL core because of the peak in $n^s(E)$, and this again would result in a contrast. In reality, the quantity $\delta = \Delta/\Gamma$ will be smaller than 1, which will reduce the contrast (§3). To eliminate the effect of spatial variations of the X-ray absorption coefficient related to structural inhomogeneities of the sample, a background image has to be subtracted which is taken for the zero-field cooled sample for which there is no FLL. In the following we denote this technique as mode 1.

Taking into account the magnetic-field-induced spin splitting of $n^n(E)$ and $n^s(E)$ we can in addition operate with an imaging mode 2 based on the X-ray magnetic circular dichroism, XMCD (Schütz *et al.*, 1987). The XMCD is based on the fact that the local absorption coefficient for circularly polarized X-rays depends on the local magnetization in the sample. Since close to E_F the spin-split density of states $n^n(E)$ is again different from the spin-split density of states $n^s(E)$, there will be an absorption contrast for circularly polarized X-rays between the FLs and the superconducting matrix (again the background image has to be subtracted). This field-induced XMCD imaging requires working at high fields which is only possible in superconductors with high H_{c2}.

3. A simple estimate for the contrast

For the imaging mode 1 we give a rough estimate of the absorption contrast $C(E)$,

$$C(E) = [\mu^n(E) - \mu^s(E)]/\mu^n(E), \tag{1}$$

where μ^n and μ^s denote the X-ray absorption coefficients in the normal-conducting and in the superconducting state. In the following we assume that the width of the absorption line is dominated by the natural linewidth determined by the core-hole lifetime whereas the instrumental linewidth is smaller. The absorption signal may be calculated *via* (Filipponi, 2000)

$$\mu^{s,n}(E) = \int \mu_0^{s,n}(E')\, L^{s,n}(E - E')\, \mathrm{d}E'. \tag{2}$$

Here, $\mu_0^{s,n}(E')$ describes the absorption which would arise for infinite lifetime of the core hole, and $L^{s,n}(E - E')$ is an appropriate broadening function. We assume the same Lorentzian broadening function for the normal-conducting and the superconducting state,

$$L^{s,n}(E - E') = \frac{1}{\pi\Gamma}\frac{1}{[(E - E')/\Gamma]^2 + 1}, \tag{3}$$

with the natural linewidth $\delta E = 2\Gamma$. The quantities $\mu_0^{s,n}(E)$ are calculated according to Fermi's golden rule,

$$\mu_0^{s,n}(E) \sim |M_{fi}^{s,n}(E)|^2 n^{s,n}(E), \tag{4}$$

where $M_{fi}^{s,n}(E)$ is the matrix element for the photoelectron transition between the initial core state i with energy E_c and the final quasiparticle valence state f at energy $E_c + E$.

To estimate the contrast for mode 1 we neglect the spin splitting of n^s and n^n (which is certainly justified when making the estimate for small external fields). The integrations in equation (2) have to be performed over the whole energy range for which $n^{s,n}(E)$ is non-zero. This would require the knowledge of $n^{s,n}(E)$ and $M_{fi}^{s,n}(E)$ for this range. However, the contrast $C(E)$ originates mainly from an energy range of the order of 2Δ around the upper gap edge, because only in that range are $n^s(E)$ and $n^n(E)$, or $M_{fi}^s(E)$ and $M_{fi}^n(E)$, drastically different (see Fig. 1), or different. In the following we assume $M_{fi}^s(E) = M_{fi}^n(E)$ for that energy range. Furthermore, we approximate $n^n(E)$ in that range by a constant $n^n(E_F)$. For $n^s(E)$ we insert the BCS quasiparticle density of states,

$$n^s(E - E_F) = \begin{cases} n^n(E_F)(E - E_F)/\left[(E - E_F)^2 - \Delta^2\right]^{1/2} & \text{for } E \geq E_F + \Delta \\ 0 & \text{otherwise} \end{cases} \tag{5}$$

which is an appropriate ansatz for a conventional superconductor. For a high-temperature superconductor both $n^n(E)$ in the very narrow FL core and $n^s(E)$ in the superconducting matrix certainly have more complicated forms. We nevertheless think that even in that case we can make a very rough estimate of the contrast with our simple assumptions. For the calculations of the integral (2) we then extrapolate these ansatzes to energies outside the relevant energy range of 2Δ, and this does not induce an appreciable error because, anyway, the contrast originates dominantly from the relevant range. Because of the same reason we can refrain from the introduction of a cut-off energy and can integrate up to infinity.

With all the above-described assumptions we obtain

$$C(\varepsilon, \delta) = [I^n(\varepsilon) - I^s(\varepsilon)]/I^n(\varepsilon), \tag{6}$$

with

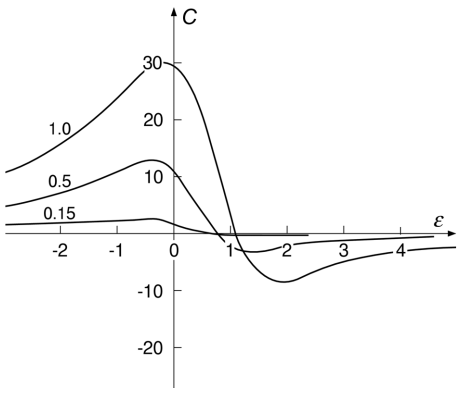

Figure 2
The contrast C (in %) as a function of the scaled energy $\varepsilon = (E - E_F)/\Gamma$ for various values of the scaled gap parameter $\delta = \Delta/\Gamma$.

$$I^{n}(\varepsilon) = \int_{0}^{\infty} \frac{d\varepsilon'}{(\varepsilon' - \varepsilon)^2 + 1} = \frac{\pi}{2} + \arctan\varepsilon \tag{7}$$

and

$$I^{s}(\varepsilon) = \int_{\delta}^{\infty} \frac{\varepsilon' d\varepsilon'}{[\varepsilon'^2 - \delta^2]^{1/2}\left[(\varepsilon' - \varepsilon)^2 + 1\right]},$$

$$\varepsilon = (E - E_F)/\Gamma, \tag{9}$$

$$\delta = \Delta/\Gamma. \tag{10}$$

The integral $I^{s}(\varepsilon)$ has to be calculated numerically. Obviously the contrast is determined just by the two scaled parameters ε and δ.

Fig. 2 shows the contrast as a function of the (scaled) irradiated X-ray energy ε for various values of the (scaled) energy gap δ. As discussed in §2, the contrast changes from positive (then the absorption in the core of the FL is larger than in the superconducting matrix) to negative when increasing the energy beyond the gap edge. The contrast decreases with decreasing δ, and for small δ the contrast is strongest for negative ε, *i.e.* when irradiating with an energy below the upper gap edge.

For the imaging mode 2 it is much more complicated to estimate the contrast. A field-induced XMCD effect becomes observable in a paramagnetic metal with large susceptibility for fields larger than 10 T (Mankowky & Ebert, 2004). It therefore may be that an XMCD contrast for the FLL would be observable in high-temperature superconductors at such fields.

4. Remarks on the realisation of the new imaging technique

For a realisation of the new imaging technique, two partly conflicting demands have to be fulfilled. First, the ratio $\delta = \Delta/\Gamma$ should not be too small (Fig. 2) and, second, the spatial resolution Δx of the X-ray microscope should be about the linear extension 2ξ of the FL core. To fulfil the first demand, one of the cuprate superconductors should be used with $2\Delta \simeq 60$ meV and 2ξ of the order of several nm. To get a feeling for the possible values of δ we consider the high-T_c superconductor YBCO. The natural linewidths are 70 meV for the M_5 edge of Y ($E = 155$ eV), 150 meV for the K edge of O (530 eV) and 0.4 eV for the L_3 edge of Cu ($E \simeq 933$ eV), corresponding to $\delta = 0.86$, 0.4 and 0.15. According to Fig. 2 this would yield a maximum contrast of about 25% for Y M_5, 10% for O K and 2% for Cu L_3, and from this point of view it would be preferable to use the M_5 edge of Y. However, with increasing X-ray energy, Δx decreases (at least for lensless imaging techniques), and for energies much smaller than 1000 eV it is probably not possible to achieve a spatial resolution of the order of 2ξ in YBCO. As a compromise, we therefore suggest using the L_3 edge of Cu which means that a very intensive X-ray source should be used to cope with the small contrast of about 2%. For the Cu L_3-edge X-ray energy of 933 eV, one way to obtain the required spatial resolution of 5 nm might be the use of lensless imaging techniques based on coherent X-ray diffraction (Marchesini *et al.*, 2003) yielding primarily results in k space. However, if a resolution of 5–10 nm is achieved by using advanced diffractive X-ray optics, *e.g.* employing higher-order zone plates (Schneider, 2003), a real-space image with a large field of view of several μm can be reached. This will be a precondition for studying the properties of defects on the FLL.

If we want to image highly irreversible dynamical processes in the FLL, a stroboscopic imaging is not possible. Instead, a 'continuous' film of the ongoing process may be produced by integrating in the detector over photon fluxes of all X-ray pulses in time windows Δt_1 followed by a respective break of the detector monitoring of Δt_2. The resolution in time (Δt_1, Δt_2) and space will then be limited by the photon flux of the available X-ray source and by the time characteristics of the detector. (If one is not primarily interested in the real-space imaging but just in the statistical properties of the FL dynamics then in certain situations a continuous wave source in combination with time-correlation techniques could be helpful.)

Altogether, we think that the imaging of the FLL by soft X-ray absorption microscopy is very demanding but probably realisable in the foreseeable future.

References

Bending, S. J. (1999). *Adv. Phys.* **48**, 449–535.
Blatter, G., Feigel'man, M. V., Geshkenbein, V. B., Larkin, A. I. & Vinokur, V. M. (1994). *Rev. Mod. Phys.* **66**, 1125–1388.
Brandt, E. H. (1997). *Phys. Rev. Lett.* **78**, 2208–2211.
Filipponi, A. (2000). *J. Phys. B*, **33**, 2835–2846.
Lozanne, A. de (1999). *Supercond. Sci. Technol.* **12**, R43–R56.
Mankovsky, S. & Ebert, H. (2004). *Phys. Rev. B*, **69**, 014414-1–014414-10.
Marchesini, S., Chapman, H. N., Hau-Riege, S. P., London, R. A., Szoke, A., He, H., Howells, M. R., Padmore, H., Rosen, R., Spence, J. C. H. & Weierstall, U. (2003). *Opt. Express*, **11**, 2344–2353.
Schneider, G. (2003). *Anal. Bioanal. Chem.* **376**, 558–561.
Schütz, G., Wagner, W., Wilhelm, W., Kienle, P., Zeller, R., Frahm, R. & Materlik, G. (1987). *Phys. Rev. Lett.* **58**, 737–740.